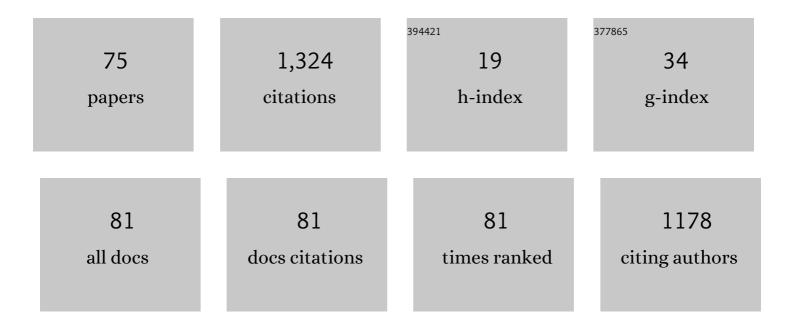
## **Michel Coret**

List of Publications by Year in descending order

Source: https://exaly.com/author-pdf/9548144/publications.pdf Version: 2024-02-01



MICHEL CODET

#	Article	IF	CITATIONS
1	FEMU based identification of the creep behavior of Zircaloy-4 claddings under simulated RIA thermo-mechanical conditions. Journal of Nuclear Materials, 2022, 561, 153542.	2.7	3
2	Nonâ€parametric stress field estimation for historyâ€dependent materials: Application to ductile material exhibiting Piobert–Lüders localization bands. Strain, 2022, 58, .	2.4	6
3	Modeling diffusive phase transformation and fracture in viscoplastic materials. International Journal of Solids and Structures, 2022, 252, 111757.	2.7	5
4	Measuring both thermal and kinematic full-fields using a single CMOS camera during high temperature tests. Optics and Lasers in Engineering, 2022, 158, 107107.	3.8	2
5	Experimental Investigation of Allotropic Transformation of Cobalt: Influence of Temperature Cycle, Mechanical Loading and Starting Microstructure. Metallurgical and Materials Transactions A: Physical Metallurgy and Materials Science, 2021, 52, 1477-1491.	2.2	6
6	The role played by viscoelasticity in the bulk material during the propagation of a dynamic crack in elastomers. International Journal of Fracture, 2021, 231, 43.	2.2	1
7	3D Hybrid Numerical Model of Residual Stresses: Numerical—Sensitivity to Cutting Parameters When Turning 15-5PH Stainless Steel. Journal of Manufacturing and Materials Processing, 2021, 5, 70.	2.2	4
8	Thermo-mechanical behavior of Zircaloy-4 claddings under simulated post-DNB conditions. Journal of Nuclear Materials, 2020, 531, 151984.	2.7	7
9	Temperature effect on strain-induced phase transformation of cobalt. Materials Letters, 2020, 281, 128812.	2.6	11
10	Experimental full field analysis for dynamic fracture of elastomer membranes. International Journal of Fracture, 2020, 224, 83-100.	2.2	10
11	Real time imaging of strain fields induced by the ferrite-to-austenite transformation in high purity iron. Materials Today Communications, 2020, 24, 101028.	1.9	4
12	Multi-partner benchmark experiment of fatigue crack growth measurements. Engineering Fracture Mechanics, 2020, 235, 107157.	4.3	2
13	Experimental study and modelling of the phase transformation of Zircaloy-4 alloy under high thermal transients. Materials Characterization, 2020, 162, 110199.	4.4	10
14	Mesoscopic Strain Fields Measurement During the Allotropic α â^' γ Transformation in High Purity Iron. Experimental Mechanics, 2019, 59, 1145-1157.	2.0	5
15	Non-parametric material state field extraction from full field measurements. Computational Mechanics, 2019, 64, 501-509.	4.0	23
16	Measuring stress field without constitutive equation. Mechanics of Materials, 2019, 136, 103087.	3.2	35
17	Reliability of the Data-Driven Identification algorithm with respect to incomplete input data. , 2019, , 311-316.		3
18	Data-based derivation of material response. Computer Methods in Applied Mechanics and Engineering, 2018, 331, 184-196.	6.6	90

MICHEL CORET

#	Article	IF	CITATIONS
19	Computational measurements of stress fields from digital images. International Journal for Numerical Methods in Engineering, 2018, 113, 1810-1826.	2.8	17
20	Validation of a multimodal setâ€up for the study of zirconium alloys claddings' behaviour under simulated <scp>LOCA</scp> conditions. Strain, 2018, 54, e12279.	2.4	7
21	Coupled Experimental/Numerical Approach to Determine the Creep Behavior of Zr-4 Cladding Under LOCA Condition. Conference Proceedings of the Society for Experimental Mechanics, 2017, , 227-230.	0.5	0
22	Affine kinematics in planar fibrous connective tissues: an experimental investigation. Biomechanics and Modeling in Mechanobiology, 2017, 16, 1459-1473.	2.8	18
23	Identification of the steady-state creep behavior of Zircaloy-4 claddings under simulated Loss-Of-Coolant Accident conditions based on a coupled experimental/numerical approach. International Journal of Solids and Structures, 2017, 115-116, 190-199.	2.7	15
24	Elasticity and symmetry of triangular lattice materials. International Journal of Solids and Structures, 2017, 129, 18-27.	2.7	13
25	Geometry of an inflated membrane in elliptic bulge tests: Evaluation of an ellipsoidal shape approximation by stereoscopic digital image correlation measurements. Medical Engineering and Physics, 2017, 48, 150-157.	1.7	5
26	Oxygen segregation in pre-hydrided Zircaloy-4 cladding during a simulated LOCA transient. EPJ Nuclear Sciences & Technologies, 2017, 3, 27.	0.7	3
27	Characterizing liver capsule microstructure via in situ bulge test coupled with multiphoton imaging. Journal of the Mechanical Behavior of Biomedical Materials, 2016, 54, 229-243.	3.1	19
28	Photobleaching as a tool to measure the local strain field in fibrous membranes of connective tissues. Acta Biomaterialia, 2014, 10, 2591-2601.	8.3	19
29	Characterisation of surface martensite-austenite transformation during finish turning of an AISI S15500 stainless steel. International Journal of Machining and Machinability of Materials, 2014, 15, 101.	0.1	13
30	Couplage entre essais et simulation en soudage. Materiaux Et Techniques, 2014, 102, 401.	0.9	0
31	A two-field modified Lagrangian formulation for robust simulations of extrinsic cohesive zone models. Computational Mechanics, 2013, 51, 865-884.	4.0	11
32	Modeling of Surface Dynamic Recrystallisation During the Finish Turning of the 15-5PH Steel. Procedia CIRP, 2013, 8, 311-315.	1.9	24
33	Robust identification of elasto-plastic constitutive law parameters from digital images using 3D kinematics. International Journal of Solids and Structures, 2013, 50, 73-85.	2.7	72
34	Compared prediction of the experimental failure of a thin fibrous tissue by two macroscopic damage models. Journal of the Mechanical Behavior of Biomedical Materials, 2013, 27, 262-272.	3.1	0
35	Comparison of two homogenization methods using a damage model for a fibrous membrane, based on the fibers' fracture process at the microscale. European Journal of Mechanics, A/Solids, 2013, 39, 1-10.	3.7	1
36	Calibration of the insert/tool holder thermal contact resistance in stationary 3D turning. Applied Thermal Engineering, 2013, 55, 17-25.	6.0	14

MICHEL CORET

#	Article	IF	CITATIONS
37	Imaging of the human Clisson's capsule by two-photon excitation microscopy and mechanical characterisation by uniaxial tensile tests. Computer Methods in Biomechanics and Biomedical Engineering, 2013, 16, 282-283.	1.6	3
38	Numerical simulation of grinding induced phase transformation and residual stresses in AISI-52100 steel. Finite Elements in Analysis and Design, 2012, 61, 1-11.	3.2	49
39	J-integral based fracture toughness of 15Cr–5Ni stainless steel during phase transformation. Engineering Fracture Mechanics, 2012, 96, 328-339.	4.3	8
40	Hybrid model for the prediction of residual stresses induced by 15-5PH steel turning. International Journal of Mechanical Sciences, 2012, 58, 69-85.	6.7	87
41	High temperature compression behavior of the solid phase resulting from drained compression of a semi-solid 6061 alloy. Materials Science & Engineering A: Structural Materials: Properties, Microstructure and Processing, 2012, 532, 37-43.	5.6	10
42	Cohesive laws X-FEM association for simulation of damage fracture transition and tensile shear switch in dynamic crack propagation. Procedia IUTAM, 2012, 3, 274-291.	1.2	6
43	Surface integrity prediction in finish turning of 15-5PH stainless steel. Procedia Engineering, 2011, 19, 270-275.	1.2	19
44	Strain Localisation and Damage Measurement by Full 3D Digital Image Correlation: Application to 15â€5PH Stainless Steel. Strain, 2011, 47, 49-61.	2.4	30
45	Characterization of the nonlinear behaviour and the failure of human liver capsule through inflation tests. Journal of the Mechanical Behavior of Biomedical Materials, 2011, 4, 1572-1581.	3.1	26
46	Shear Behavior of AA6061 Aluminum in the Semisolid State Under Isothermal and Nonisothermal Conditions. Metallurgical and Materials Transactions A: Physical Metallurgy and Materials Science, 2011, 42, 3370-3377.	2.2	7
47	Microstructural and mechanical properties evolutions of plasma transferred arc deposited NoremO2 hardfacing alloy at high temperature. Materials Science & Engineering A: Structural Materials: Properties, Microstructure and Processing, 2011, 528, 5096-5105.	5.6	11
48	Experimental study of the fracture kinetics of a tubular 16MnNiMo5 steel specimen under biaxial loading at 900 and 1000°C. Application to the rupture of a vessel bottom head during a core meltdown accident in a pressurized water reactor. Nuclear Engineering and Design, 2011, 241, 755-766.	1.7	8
49	3D Numerical Prediction of Residual Stresses in Turning of 15-5PH. Advanced Materials Research, 2011, 223, 411-420.	0.3	9
50	Hot Tearing Sensitivity of Al-Mg-Si Alloys Evaluated by X-Ray Microtomography After Constrained Solidification at High Cooling Rate. , 2011, , 87-99.		5
51	On the Use of NURBS Functions for Displacement Derivatives Measurement by Digital Image Correlation. Experimental Mechanics, 2010, 50, 1099-1116.	2.0	46
52	Mechanical Behavior of AA6061 Aluminum in the Semisolid State Obtained by Partial Melting and Partial Solidification. Metallurgical and Materials Transactions A: Physical Metallurgy and Materials Science, 2010, 41, 2257-2268.	2.2	48
53	Mechanical characterization of liver capsule through uniaxial quasi-static tensile tests until failure. Journal of Biomechanics, 2010, 43, 2221-2227.	2.1	88
54	Stable crack propagation in steel at 1173K: Experimental investigation and simulation using 3D cohesive elements in large-displacements. Engineering Fracture Mechanics, 2010, 77, 776-792.	4.3	3

#	Article	IF	CITATIONS
55	A cohesive zone model which is energetically equivalent to a gradient-enhanced coupled damage-plasticity model. European Journal of Mechanics, A/Solids, 2010, 29, 976-989.	3.7	32
56	A thermodynamic method for the construction of a cohesive law from a nonlocal damage model. International Journal of Solids and Structures, 2009, 46, 1476-1490.	2.7	65
57	A Finite Element Method for Level Sets. , 2009, , 95-106.		1
58	Étude mécanique d'un changement de phase allotropique à l'échelle mésoscopique. Materiaux Techniques, 2009, 97, 81-87.	Et 0.9	1
59	Unstable Crack Propagation Under Severe Accident Scenario Conditions in a Pressurized Water Reactor. , 2009, , .		0
60	A partitionâ€ofâ€unityâ€based finite element method for level sets. International Journal for Numerical Methods in Engineering, 2008, 76, 1513-1527.	2.8	13
61	Numerical simulation of welding induced damage and residual stress of martensitic steel 15-5PH. International Journal of Solids and Structures, 2008, 45, 4973-4989.	2.7	13
62	Study of tearing behaviour of a PWR reactor pressure vessel lower head under severe accident loadings. Nuclear Engineering and Design, 2008, 238, 2411-2419.	1.7	15
63	Numerical simulation of damage in two-scale model of stainless steel 15-5PH. European Journal of Computational Mechanics, 2008, 17, 829-841.	0.6	0
64	Strain simulation of steel during a heating-cooling cycle including solid-solid phase change. European Journal of Mechanics, A/Solids, 2007, 26, 460-473.	3.7	1
65	Methodology to determine failure characteristics of planar soft tissues using a dynamic tensile test. Journal of Biomechanics, 2007, 40, 468-475.	2.1	101
66	Comparison of two transformation plasticity models, with and without kinematic hardening for bainitic transformation under non-proportional loading path. European Physical Journal Special Topics, 2004, 120, 177-183.	0.2	0
67	Experimental study of the phase transformation plasticity ofÂ16MND5 low carbon steel induced by proportional and nonproportional biaxial loading paths. European Journal of Mechanics, A/Solids, 2004, 23, 823-842.	3.7	33
68	<title>Experiments of transformation-induced plasticity under multiaxial loadings for a 16MND5&lt;br&gt;low-carbon steel</title> . , 2002, 4537, 115.		0
69	A two scale model for the simulation of residual stresses due to welding of a metallic multiphase material. , 2002, , 981-988.		0
70	Experimental study of the phase transformation plasticity of 16MND5 low carbon steel under multiaxial loading. International Journal of Plasticity, 2002, 18, 1707-1727.	8.8	62
71	A mesomodel for the numerical simulation of the multiphasic behavior of materials under anisothermal loading (application to two low-carbon steels). International Journal of Mechanical Sciences, 2002, 44, 1947-1963.	6.7	39
72	Cracking Cohesive Law Thermodynamically Equivalent to a Non-Local Damage Model. Key Engineering Materials, 0, 385-387, 81-84.	0.4	0

MICHEL CORET

#	Article	IF	CITATIONS
73	Influence of Si and Mg Contents on the Mechanical Behavior of Al-Mg-Si Alloys in the Semi-Solid State under Isothermal and Non-Isothermal Conditions. Materials Science Forum, 0, 690, 73-76.	0.3	1
74	Numerical simulation of damage in two-scale model of stainless steel 15-5PH. European Journal of Computational Mechanics, 0, , 829-841.	0.0	6
75	Two Fields Formulations for the Implementation of an Extrinsic Cohesive Law. , O, , .		Ο